



A Numerical Investigation of the Effect of Hydrogen Blending on the Temperature Field and Polutants Emission of a Four Stroke Spark Ignition Engine

Dr. Haroun A.K. Shahad

Dr. Samir M. Abdul Haleem

**Department of Mechanical Engineering,
College of Engineering
Babylon University, Iraq**

Abstract:

The internal combustion engines are generally a major source of air pollution. However the spark ignition engines are recognized by their carbon monoxide and unburned hydrocarbon emission. One of the methods used to reduce the emission of these pollutants is the blending of hydrogen with the gasoline fuel, either on a mass basis or on energy replacement basis. The present research study is devoted to concern with developing a numerical model to predict the effect of hydrogen blending (based on energy replacement) on the emitted concentrate of carbon and nitrogen oxides and the temporal and local variation of cylinder temperature.

It is found that hydrogen blending improves combustion process by increasing the flame propagation speed and hence increasing maximum cylinder temperature. The timing of maximum cylinder temperature is also advanced due to hydrogen blending.

It is also found that the hydrogen blending reduces CO and CO₂ concentrations and increases NO_x concentrations. It is found that when the hydrogen blending ratio exceeds 20% the engine performance is deteriorated.

Keywords – hydrogen, blended fuel, spark ignition engine, pollutants, combustion.

1 Introduction

Air pollution becomes a world wide problem and needs to be solved. The solution start by identify the sources of the air pollutions and reducing or eliminating the concentration of the pollution emitted from the sources. One of the major sources of air pollutions is the spark ignitions engine. Spark ignition engines is noticed for its high concentration of carbon monoxide and unburned hydrocarbon emission. Therefore many theoretical and experimental researches are directed toward improving the combustion process of spark ignition engine and hence reducing the concentrate of the pollutants within exhaust gases.

The various engine combustion models that have been developed to date may be grouped into three categories [1]:

1. Zero dimensional models
2. Quasi-dimensional models
3. Multi-dimensional models

In the above classification, although the level of detail and proximity to physical reality increases as one precedes downward, so does the complexity of creating and using those models.

Multi-zone models (which considered in the present study) take this form of analysis one step further by considering energy and mass balances over several zones, thus obtaining results that are closer to reality.

The aim of the present work is to study the performance and emissions of a single cylinder air cooled spark ignition engine operated with gasoline enriched hydrogen. However many researches had been directed toward engines operated with hydrogen blended fuel, pollutant, performance and components.

Prabhu et al, [2], 1985, developed an analytical model to study the performance, fuel economy and nitric oxide emission of a supercharged spark ignition hydrogen engine. In this work, a quasi one dimensional model was developed. The semi empirical turbulent flame speed expression suggested by Fagelson was used.

$$U_T = A * Re^B * U_L \quad (1)$$

In which A and B are empirically determined constants, Re is the Reynolds number based on the piston diameter, mean piston speed, and the burnt gas properties, and U_L is the laminar flame speed. They found that:

1. By supercharging the hydrogen engine the knock limit was set in at an equivalence ratio leaner than the naturally aspirated hydrogen engine.
2. The indicated power increases for supercharging pressure when compared with the naturally aspirated engine.
3. Compared to naturally aspirated engine at an equivalence ratio of 0.4 the indicated thermal efficiency increases.
4. NO emission increase by supercharging. The peak level of NO emissions occurs at an equivalence ratio of 0.8 for naturally aspirated engine and at about 0.77 for supercharged conditions.

Shahad and Sadiq, [3], 1999, developed a quasi-dimensional model to study the effect of hydrogen blending on fuel consumption and pollutant concentrations. Investigations had been concentrated on decreasing fuel consumption by using alternative fuels and on lowering the concentration of toxic components in combustion products. They concluded that

1. The hydrogen added to gasoline engine improves the combustion process, especially in the later combustion period, reduces the ignition delay, speed up the flame front propagation, reduces the combustion duration and retards the spark timing.
2. The thermal efficiency of the engine is increased until a hydrogen-fuel mass ratio of 8% of stoichiometric mixture and 10% for 0.8 equivalence ratio.
3. The concentration of CO is reduced and the concentration of NOx is increased due to hydrogen blending.
4. The peak pressure and temperature increase, and the pressure diagram gets closer to the ideal diagram.
5. The power is increased until hydrogen-fuel mass rate of 2% for stoichiometric mixture and 10% for 0.8 equivalence ratio.

Das, et al, [4], 2000, evaluated the potential of using a clean-burning fuel such as hydrogen for a small horsepower spark ignition engines since (CNG) has already been used as an alternative fuel for internal combustion. An effort had been made in the present work to compare hydrogen selling with CNG operation. The engine was operated separately either with hydrogen or compressed natural gas using an electronically-controlled, solenoid-actuated injection system developed in the engine and unconventional laboratory of the Indian Institute of Technology, Delhi. It had been observed that the brake specific fuel consumption was reduced and the brake thermal

efficiency improved with hydrogen operation compared to systems running on compressed natural gas.

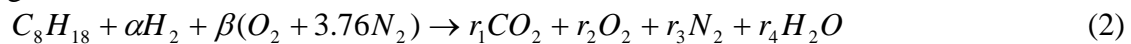
Hailin and Karim, [5], 2003, employed a quasi-dimensional two-zone model for the operation of spark ignition engine when fueled with hydrogen. A knock prediction model, developed previously for spark ignition engine methane-hydrogen fueled engine applications was extended to consider operation on hydrogen. The effects of changes in operation conditions include a very wide range of variations in equivalence ratio on the onset of knock and its intensity, combustion duration, power, efficiency and operational limits were investigated. They found that the compression ratio and intake temperature are the main parameters that affect the knock limited equivalence ratio while the effect of spark timing tend to be in comparison less effective. The knock free operational mixture region tends to narrow significantly with increasing compression ratio and intake temperature. This represents a practical limitation to the improvement of power and efficiency of hydrogen engines.

However many research programs were recently carried out to study the performance of hydrogen engine [6], [7], [8], [9], [10], [11]. It is found that pure hydrogen can be used as a fuel for gasoline engines with slight increase in compression ratio due to the high self ignition temperature of hydrogen. The only pollutant in this case is the nitrogen oxide if air is used. However the pollutants are emitted when pure oxygen is used.

It must be stressed that in this work the mixing process is based on energy bases rather than on mass bases, where the amount of hydrogen energy added is equal to the amount of hydrocarbon energy removed. It is thought that this mixing process given better assessment of the blending process.

2 Mathematical Model

The reaction equation of the complete combustion of hydrogen blended gasoline fuel is written as follows.



2.1 Zone Generation

The whole charge in the cylinder is divided into layers of equal height. Each layer is divided into nn (10) circumferential ring elements, each ring element is divided into 360 zones (each one degree) as shown in figure (1). So the element thickness (d) is a function of cylinder bore (b)

$$d = \frac{b/2}{10} \quad (3)$$

Assuming the zone has a square profile, i.e. the height equal the thickness, thus the number of rows of zones in the z direction (mm) is equal to

$$mm = \frac{(s + \frac{4V_c}{\pi b^2})}{d} \quad (4)$$

Where V_c is the clearance volume. The volume of each element is a function of its location as

$$V(ii, jj, kk) = \pi * 0.1 * ii * b * d^2 / 360 \quad (5)$$

Where $ii = 1, nn(10)$

$$jj = 1, mm$$

$$kk = 1, 360$$

The summation of volumes of all zones at each time (crank angle) step must equal to the total cylinder volume

$$V_{cyl}(\theta) = \sum_{ii=1}^{nn} \sum_{jj=1}^{mm} \sum_{kk=1}^{360} V(ii, jj, kk) \quad (6)$$

Also the summation of masses of all zones equal to the total mass of the cylinder, thus [12]

$$m_{cyl} = \sum_{ii=1}^{nn} \sum_{jj=1}^{mm} \sum_{kk=1}^{360} m(ii, jj, kk) \quad (7)$$

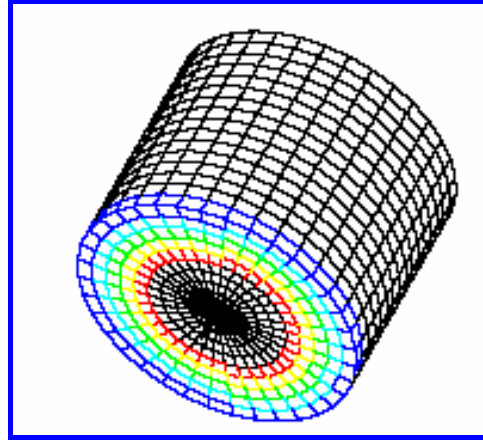


Figure (1) Incylinder Zonal Distribution [12]

2.2 Heat Transfer Model:

Heat flux into the walls varies through the engine cycles from negative to positive values reaching up to several megawatts per square meter. Also varies spatially due to differences in local gas temperature and velocity and doubles also due to differences in orientation of the wall to the radiating flames.

2.2.1 Convective Heat Transfer

Woschni developed the power of 0.8 empirical equation for forced convection heat transfer as

$$Nu = 0.035 Re^{0.8} \quad (8)$$

Woschni proposed an empirically based in which the characteristic velocity term (local average gas velocity) is expressed as [13]

$$w = C_3 Sp + C_4 \left(\frac{V_d T_{ref}}{P_{ref} V_{ref}} \right) (P - P_{mot}) \text{ [m/s]} \quad (9)$$

Where

Sp, P, P_{mot} piston speed, cylinder pressure, and motor pressure

P_r, V_r, T_r working fluid pressure, volume, temperature at some reference condition (inlet valve closing)

C_3 and C_4 are model constant, which are specified as [14]

For compression period

$$C_3=2.28 \quad C_4=0$$

For combustion and expansion period

$$C_3=6.18 \quad C_4=3.24 \times 10^{-3}$$

With the cylinder bore (b) taken as the characteristic length

2.2.2 Radiative Heat Transfer

2.2.2.1 Total Gas Emissivity

The non luminous radiation from the combustion gases is primarily due to emission contributions from the tri-atomic molecules of carbon dioxide, water vapor. Thus the total gas emissivity may be calculated by the following approximation [15].

$$\varepsilon_g = \varepsilon_{CO_2} + \varepsilon_{H_2O} - \varepsilon_{CO_2} \varepsilon_{H_2O} \quad (10)$$

The emissivity of carbon dioxide and water vapor can be calculated by the following empirical relations:

$$\varepsilon_{CO_2} = \frac{0.711(p_{CO_2} l_{rad})^{1/3}}{(T_{ij}/100)^{1/2}} \quad (11)$$

$$\varepsilon_{H_2O} = \frac{0.707(p_{H_2O} l_{rad})^{1/3}}{(T_{ij}/100)^{1/2}} \quad (12)$$

where p_{CO_2} partial pressure of (CO₂) [bar]
 p_{H_2O} partial pressure of (H₂O) [bar]
 T_{ij} temperature of zone (i, j) [K]

The mean path length of a volume V and a surface area A is given with sufficient accuracy by [14]

$$l_{rad} = 0.9 \frac{4V}{A} \quad (13)$$

2.2.2.2 Direct and Total Exchange Area Factors

Assume the surface of the equivalent cylinder includes the cylinder linear, the head of the cylinder, and the piston crown. The charge is broken into about (1*10⁵) element as shown in section (3.3.4). Eight types of direct exchange area factors are calculated during each time step and they are

1. Cylinder linear to cylinder head direct exchange area.
2. Cylinder linear to piston crown direct exchange area.
3. Cylinder linear to itself direct exchange area.
4. Piston crown to cylinder head direct exchange area.
5. Gas element to cylinder linear direct exchange area.
6. Gas element to piston crown direct exchange area.
7. Gas element to cylinder head direct exchange area.
8. Gas element to gas element direct exchange area.

This is the direct exchange area between the different gas elements.

The surface is broken into N isothermal elements while the medium is broken into k isothermal volumes.

Where the subscripts *s* and *g* are used to distinguish between the emissive power and irradiation of surface element and volume zone, respectively.

Making an energy balance over a volume zone, have [12, 16].

$$Q_{gi} = \kappa V_i (4Eb_{gi} - G_i) \quad (14)$$

$$Q_{gi} = \sum_{j=1}^N s_j g_i (Eb_{gi} - J_j) + \sum_{k=1}^K g_k g_i (Eb_{gi} - Eb_{gk}) \quad (15)$$

$$Q_{gi} = 4\kappa V_i Eb_{gi} - \sum_{j=1}^N \overline{s_j g_i} J_j - \sum_{k=1}^K \overline{g_k g_i} Eb_{gk}, i = 1, 2, \dots, K \quad (16)$$

Looking to an isothermal enclosure, found that

$$\sum_{j=1}^N \overline{s_j g_i} - \sum_{k=1}^K \overline{g_k g_i} = 4\kappa V_i, i = 1, 2, \dots, K \quad (17)$$

For a volume zone the Q_{gi} represent the net radiative source within volume V_i and is, therefore,

$$Q_{gi} = \int_{V_i} A \cdot q dV_i \quad (18)$$

$$Q_{gi} = 4\kappa V_i Eb_{gi} - \sum_{j=1}^N \overline{s_j g_i} J_j - \sum_{k=1}^K \overline{g_k g_i} Eb_{gk}, i = 1, 2, \dots, K \quad (19)$$

2.3 Mechanism of Flame

The combustion process in the spark ignition engine takes place in a turbulent flow field [13]. Unlike a laminar flame, which has a propagation velocity that depend unequally on the thermal and chemical properties of the mixture, a turbulent flame has a propagation velocity that depends on the characteristics of the flow, as well as the mixture properties. Turbulent flame speed (U_t) can be defined as the velocity at which the unburned mixture enters the flame front in a direction normal to the flame [17].

The essential features of the flame development and propagation processes are described as

1. The flame development angle: the crank angle interval between the spark discharge and the time when a small fraction of the cylinder mass has burned. Usually this fraction equal to (0.1 percent) of cylinder volume. Hence the development period is [13, 17]

$$Dp = \frac{6RPM}{U_t} \sqrt[3]{\frac{0.001V_{cyl}}{\pi}} \quad (20)$$

2. Rapid-burned angle: the crank angle interval required to burn the bulk of the charge. Its defined as the interval between the end of the flame development and the end of flame propagation process

The laminar flame velocity for mixture of gasoline and hydrogen fuel in spark ignition is modeled as [6]

$$Ul = 9656 \left(\frac{P}{P_o} \right)^{-0.623} e^{\frac{-2145}{T_u}} + 0.83Y_{H_2} \quad (21)$$

P_o reference pressure [bar]

And

$$Y_{H_2} = \left[\frac{[H_2] + \frac{[H_2]}{[H_2/air]_{st}}}{[G] + [air] - \frac{[H_2]}{[H_2/air]_{st}}} \right] \quad (22)$$

where

$[H_2]$ is the molecular concentration of hydrogen

$[G]$ is the molecular concentration of gasoline

$[air]$ is the molecular concentration of air

$[H_2 / air]_{st}$ is the stoichiometric ratio of hydrogen concentration to air concentration

Laminar flame speed is affected by the residual gas from the previous cycle in combustion chamber. Heywood [14] show that

$$Ul = Ul(1 - 2.06Xb^{0.77}) \quad (23)$$

where Xb is the mole fraction of diluents of the burned gas.

Therefore the turbulent flame front speed is described as [18]

$$Ut = Ul * ff \quad (3.151)$$

Where ff is the turbulization factor which can be taken proportional to engine speed [14, 19]

$$ff = 1 + 0.0018RPM \quad (24)$$

2.4 Nitric Oxides Formation:

Nitric oxide is an important minor species in combustion because of its contribution to air pollution. In the combustion of fuels that contain no nitrogen, nitric oxide is formed by three chemical mechanisms or routes that involve nitrogen from the air which are: The thermal or Zeldovich mechanism, the Fenimov or prompt mechanism, and the N_2O - intermediate mechanism [1, 17]. The thermal (Zeldovich) mechanism dominates in high temperature combustion over a fairly wide range of equivalence ratio [20, 13, and 17].

2.5 Overall cylinder Temperature and Pressure:

The overall cylinder temperature is obtained as follows

$$T_{overall} = \frac{\sum_{ii=1}^{nm} \sum_{jj=1}^{mm} \sum_{kk=1}^{360} m(ii, jj, kk) T(ii, jj, kk)}{m_{cyl}} \quad (25)$$

thus,

$$\frac{P_{cyl} V_{cyl}}{RT_{overall}} = \sum_{ii=1}^{nm} \sum_{jj=1}^{mm} \sum_{kk=1}^{360} \frac{P(ii, jj, kk) V(ii, jj, kk)}{RT(ii, jj, kk)} \quad (26)$$

or the new cylinder pressure becomes

$$P_{cyl} = \frac{RT_{overall}}{V_{cyl}} \sum_{ii=1}^{nm} \sum_{jj=1}^{mm} \sum_{kk=1}^{360} \frac{P(ii, jj, kk) V(ii, jj, kk)}{RT(ii, jj, kk)} \quad (27)$$

2.6 Combustion process

The combustion process starts as the spark plug fired. The flame expands and travels across the chamber until finally the whole of the mixture is engulfed by flame. The combustion chamber is divided into many layers of ring elements; each layer contains ten rings. Each ring element is broken into 360 elements. The flame front travels in a surface of a hemispherical shape assumed of thickness equal to the mesh size. The combustion process occurs only in the zones that lie on the flame front (the hemispherical surface) except the dissociation processes which continuous in the back flame zones.

The convection heat transfer between each ring element and its neighbors is calculated. The radiation heat transfer between each zone and all other zones, cylinder linear, cylinder head and piston crown are calculated at each time step.

The time step or crank angle step (in the combustion process) is the time required for the flame to travel a zonal thickness. Thus the time increment is

$$\Delta t = \frac{\sqrt{2}.d}{U_t} \quad (28)$$

So the crank angle increment becomes

$$\Delta \theta = 6.RPM\Delta t \quad (29)$$

3 Results and Discussions

3.1 Effect of Hydrogen Addition on Flame Speed

The effect of hydrogen addition on flame speed history along the cylinder centerline is shown in figures (2) and (3) at air to fuel ratio of 14 and 16 respectively. It is clearly shown that the blending of hydrogen enhances the flame speed. The reason behind that is the enhancement of mixing process due to the presence of hydrogen and hence shorter combustion process. It's clear that the flame speed becomes at minimum value slightly after top dead center. By comparing the flame speed with the pressure diagram history, it can be found that the minimum flame speed occur at the maximum cylinder pressure. The minimum value of flame speed occurs earlier as hydrogen blending ratio is increased. This is due to the increase in flame speed that reduces the combustion duration so the maximum cylinder pressure occurs earlier. By comparing figures (2) and (3) it's clearly shown that the flame speed at air to fuel ratio 14 is greater than the flame speed at 16 air to fuel ratio.

3.2 Effect of Hydrogen Addition on the Zonal Temperature Distribution

Figures (4, 5, and 6) show the isothermal contours for 0%, 10% and 20% blended hydrogen respectively, at 14 air to fuel ratio, and 180° C.A. The contours show the flame front propagation and the temperature distribution in the engine cylinder. The temperature reductions downstream the flame front has the same shape of the flame propagation history. This is due to the heat transfer from the zones and the equal period of time available for the zones that leave the flame surface at the same moment. It's clear that as the hydrogen blending ratio increases, the flame speed will also increase, so the time of flame traveling through the cylinder decreases, and the combustion duration becomes shorter. The figures show that the maximum local temperature is at the flame front. The temperature decreases on both side of the flame front (upstream in the gas zones and down stream in the unburnt mixture zones). The figures also shows that the flame travels faster as the blending ratio increases where it hits the piston crown at 20% blending ratio, since the presence of hydrogen enhance the flame speed.

3.3 Overall Cylinder Temperature

The effect of hydrogen blending on the history of the mean cylinder temperature is also studied. Figure (7) shows the effect at an engine speed at 2000 rpm and a compression ratio of 6.5 and air to fuel ratio of 14. The results show that, although the energy input is the same, for all cases, the peak mean cylinder temperature is increased and advanced. This is due to the increase of flame propagation speed. However the increase in the mean cylinder temperature is more pronounced with stoichiometric mixture.

3.4 In-cylinder Nitric Oxides

Figure (8), gives the in-cylinder mean concentration of nitric oxides as a function of crank angle for different hydrogen blending ratios of a naturally aspirated engine with a compression ratio of 6.5 and an engine speed of 2000 rpm. The air to fuel ratio is 14. It is clearly shown that the blending of hydrogen increases the amount of nitric oxides concentration. This is attributed to the high burning temperature of hydrogen-blended. There are decreases in the amount of nitric oxides through the expansion period due to reduction in the contents temperature that lead the back reaction occurred.

3.5 Effect of Hydrogen Addition on Exhaust Gas Emissions

Figures (9) and (10) show the CO₂ and CO emissions as a function of air to fuel ratio with different hydrogen addition ratios for a naturally aspirated engine with 6.5 compression ratio, and 2000 rpm engine speed.

For pure gasoline the CO₂ emission is maximum slide to the lean side. The CO₂ emission decreases as hydrogen blending ratio increases, that due to the replacement of hydrocarbon fuel by hydrogen.

Figure (10) shows the increase in the CO emission level in the exhaust gas with the decrease in the air to fuel ratio. For rich mixture CO level is higher because complete oxidation of fuel carbon to CO₂ is not possible due to insufficient oxygen. For lean side the CO emission concentration varies little with the air to fuel ratio. It's clearly shown that hydrogen addition reduces the CO concentration. This is due to the reduction in the hydrocarbon as hydrogen replacement.

Figure (11) gives the nitric oxides concentration as a function of the air to fuel ratio at different hydrogen blending ratios. In general for pure gasoline, the peak nitric oxides emission occurs on the weak side at air to fuel ratio of about 16, and falls off considerably over a few air to fuel ratios. The higher the peak temperature the higher the nitric oxide concentration and the lower the flame speed the longer time for nitric oxide to dissociate to N₂ and O₂. Thus any factor reduces the peak temperature or decreases the flame speed or both will reduce the NO emissions. The increase in the hydrogen blending ratio leads to an increase in the nitric oxides emissions, that's due to the increase in the end gas temperature and increasing the flame speed as hydrogen blending ratio increases. The maximum nitric oxides concentration slides to the rich mixture side as the increase in the temperature by hydrogen addition has a greater effect in the rich air to fuel ratio than in the lean mixture and the more oxygen available if hydrogen replacement due to lower consumption of oxygen by hydrogen compared to gasoline as energy replacement.

Figure (12) gives the oxygen concentration with respect to air to fuel ratio for different hydrogen blending ratios. It's clearly shown that increasing richness interprets to expend the most oxygen in the combustion chamber, so the oxygen concentration is lower in the rich mixture. The hydrogen blending increases the oxygen concentration as hydrogen consumes oxygen lower than gasoline for same input heat.

3.6 Effect of Hydrogen Addition on Engine Performance

Figures (13), (14), (15), and (16) show the effect of air to fuel ratio at different hydrogen blending ratios on the thermal efficiency, the brake mean indicated pressure, the indicated power, and the specific fuel consumption, respectively. The figures are

drawn for a naturally aspirated engine with 6.5 compression ratio, and 2000 rpm engine speed.

The thermal efficiency for pure gasoline operation is at maximum value at air to fuel ratio about 16 (lean mixture). Its noticeably that the blended hydrogen improve efficiency, that's due to the increase in the cylinder content temperature, also increasing blended hydrogen fasten the flame speed so the pressure diagram approach to the ideal diagram. The maximum value of the thermal efficiency slid to the rich side as blended hydrogen increase, the reason behind that is the effect of blended hydrogen on flame speed is greater in the rich mixture than that for lean mixture. The engine thermal efficiency is also improved as the percentage of hydrogen blending is increased reaching maximum at about 20% blending. With further increase in hydrogen blending the thermal efficiency decrease is due to the drop in the volumetric efficiency. The reason behind the drop in the volumetric efficiency as hydrogen blending ratio increase is the low density of hydrogen compared to gasoline that cause a reduction in the mixture density which reduce the volumetric efficiency.

The brake mean indicated pressure and indicated power are increase as increase mixture richness, that due to increase in amount of fuel bunt. Enlarge the ratio of hydrogen blended increase the indicated mean effective pressure, the reason behind that is the reduction of the time of combustion process due to rate the flame propagation speed, so the pressure diagram becomes close to the ideal diagram. The high blended ratio (about 20%) gives small increased in the brake mean indicated pressure and so the indicated power, that because of the low density of hydrogen that drop off the volumetric efficiency.

The specific fuel consumption is at minimum value at lean mixture (air to fuel ratio of 16) and decreases as increasing the hydrogen blending ratio, that's due to the increase in engine isothermal efficiency. The minimum specific fuel consumption shift to the hydrogen blending ratio, that's because of the high increase in flame speed for rich mixture rather than the lean mixture.

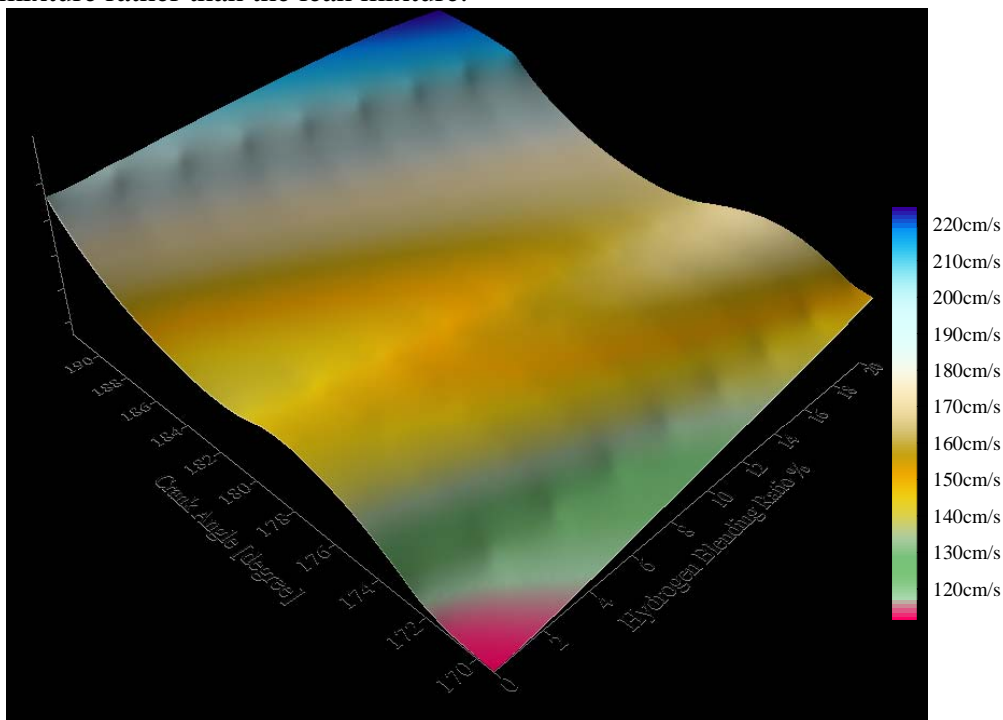


Figure (2) The Effect of Hydrogen Blending Ratio on the Flame speed at AFR=14, C.R.=6.5, and an Engine Speed of 2000 rpm

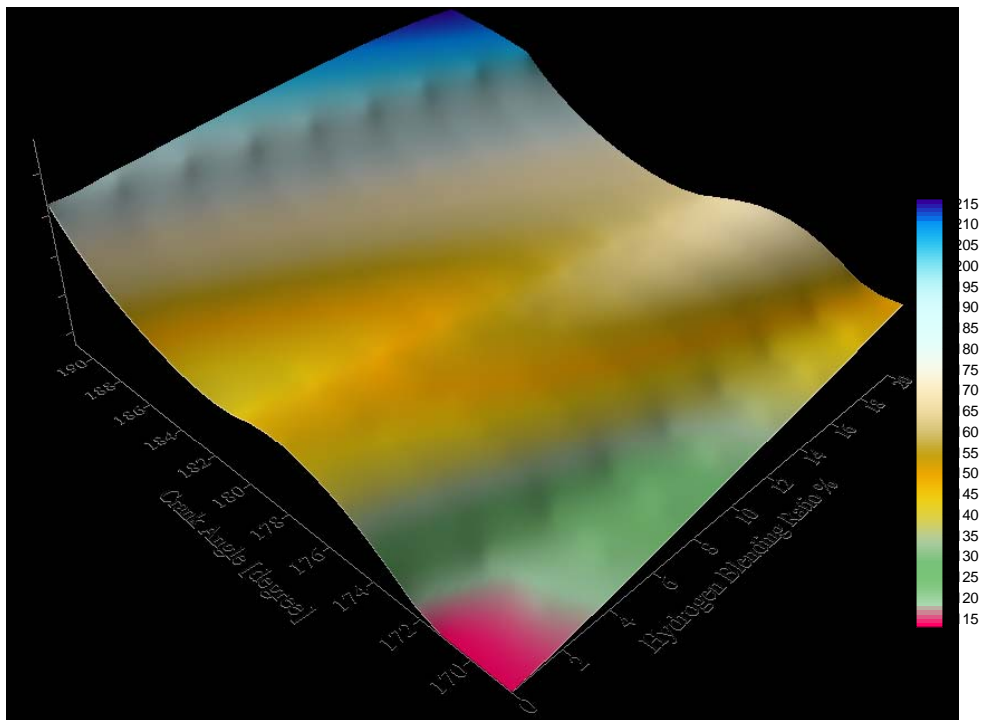


Figure (3) The Effect of Hydrogen Blending Ratio on the Flame speed at AFR=16, C.R.=6.5, and an Engine Speed of 2000 rpm

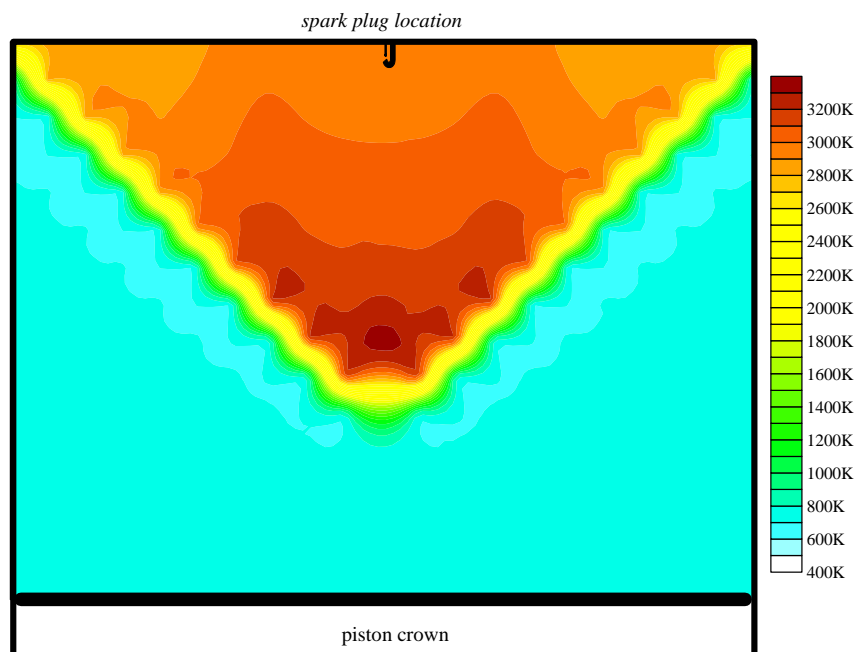


Figure (4) Incylinder Isothermal Contours at 2000 rpm, AFR= 14, 180 degree C.A. (pure gasoline)

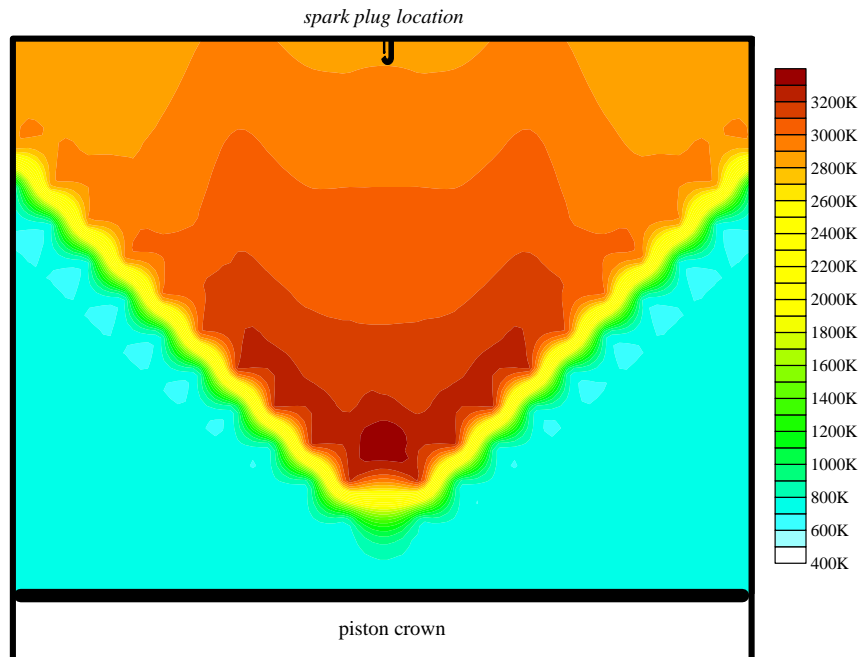


Figure (5) Incylinder Isothermal Contours at
2000 rpm, AFR= 14, 180 degree C.A.
(10 % blended hydrogen)

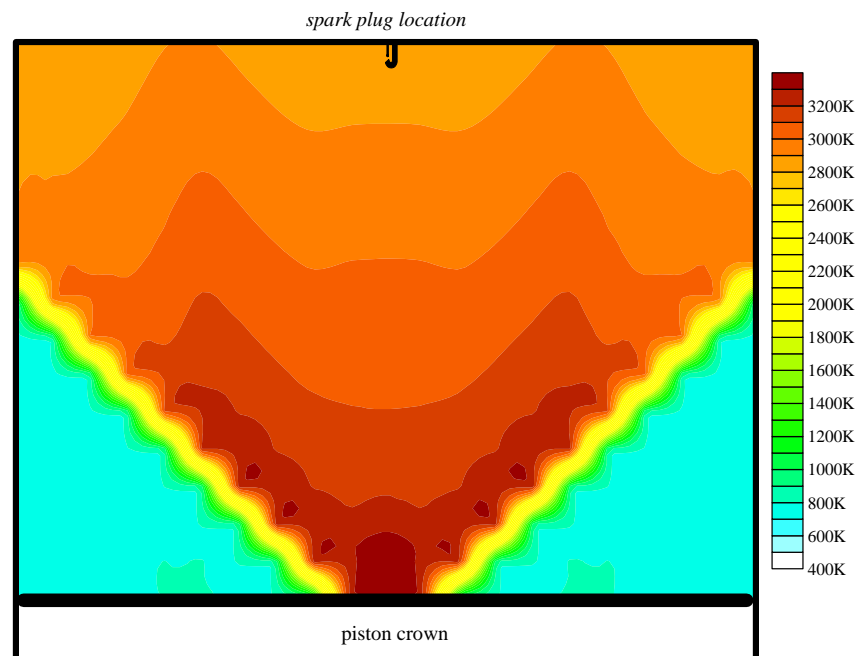


Figure (6) Incylinder Isothermal Contours at
2000 rpm, AFR= 14, 180 degree C.A.
(20% blended hydrogen)

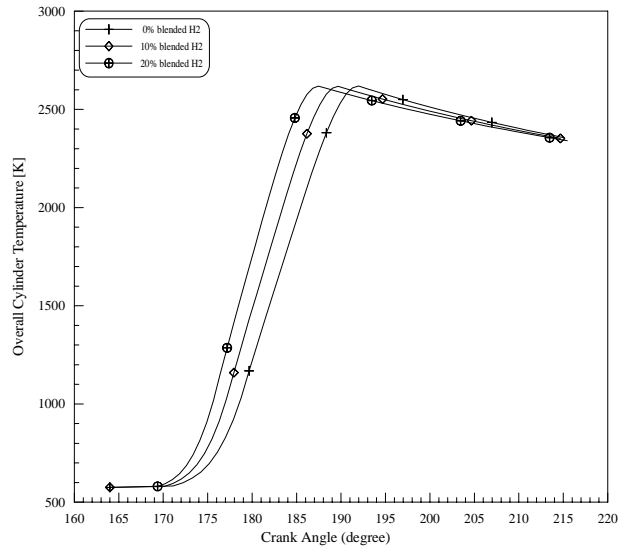


Figure (7) Effect of Hydrogen Addition on Overall Cylinder Temperature
AFR=14, 2000 rpm, C.R.=6.5

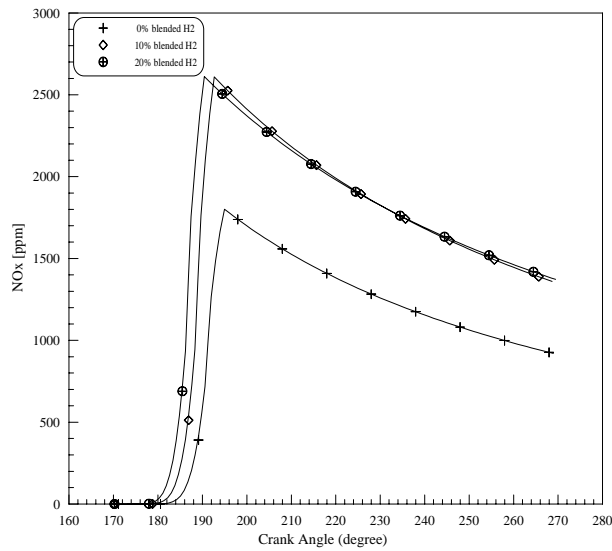


Figure (8) Effect of Hydrogen Addition on NOx Concentration
AFR=14, 2000 rpm, C.R.=6.5

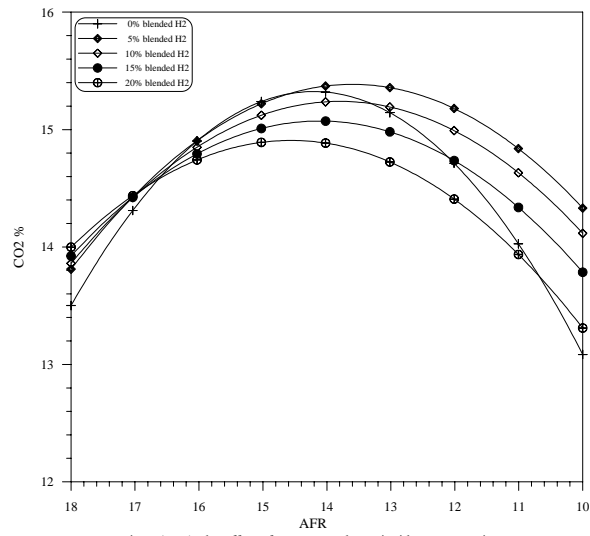


Figure (9) The Effect of AFR on Carbon Dioxide Concentration for Different Hydrogen Blending Ratio
AFR=14, 2000 rpm, C.R.=6.5

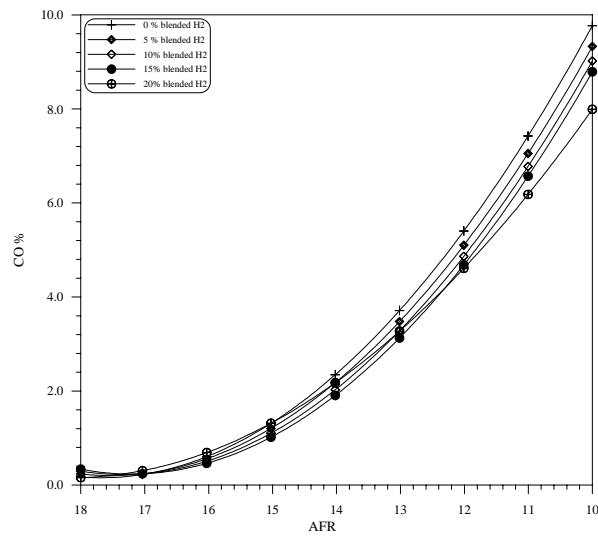


Figure (10) The Effect of AFR on Carbon Monoxide Concentration for Different Hydrogen Blending Ratio
AFR=14, 2000 rpm, C.R.=6.5

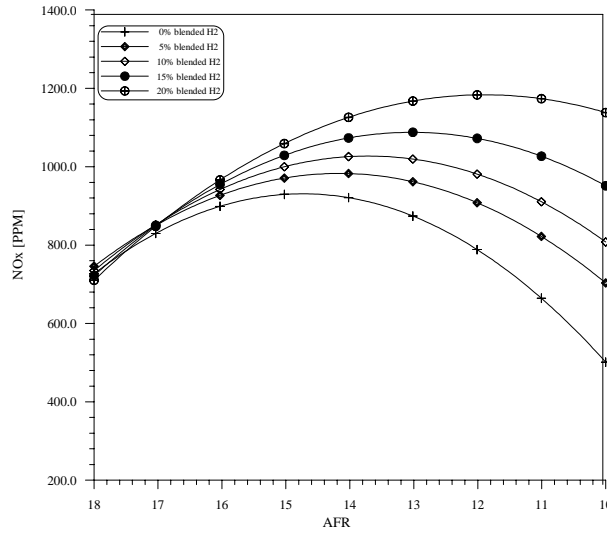


Figure (11) The Effect of AFR on Nitric Oxide Concentration for Different Hydrogen Blending Ratio
AFR=14, 2000 rpm, C.R.=6.5

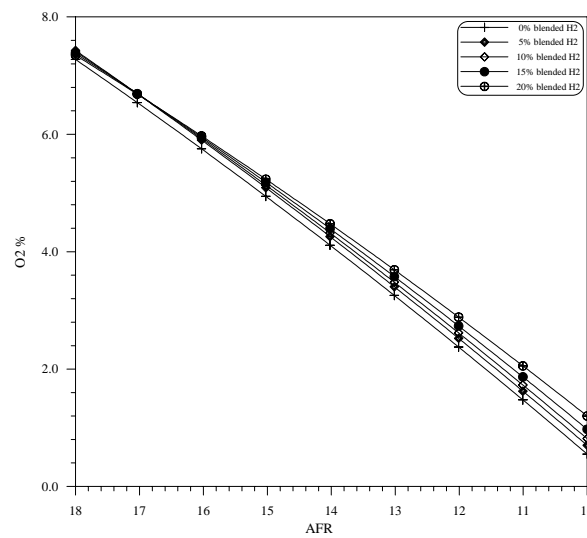


Figure (12) The Effect of AFR on Oxygen Concentration for Different Hydrogen Blending Ratio
AFR=14, 2000 rpm, C.R.=6.5

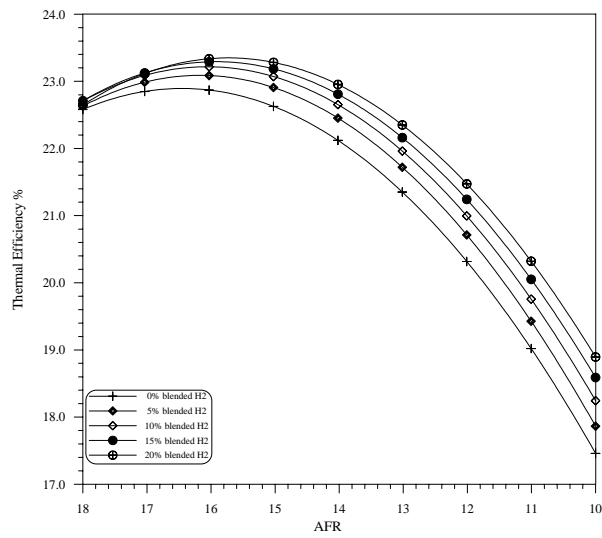


Figure (13) The Effect of AFR on Thermal Efficiency for Different Hydrogen Blending Ratio
AFR=14, 2000 rpm, C.R.=6.5

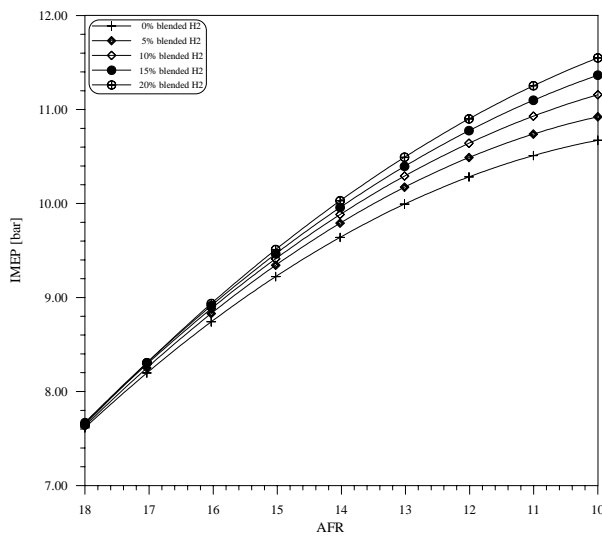
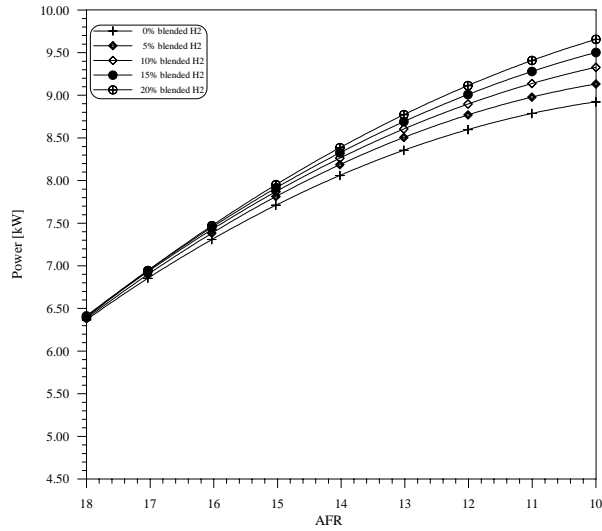
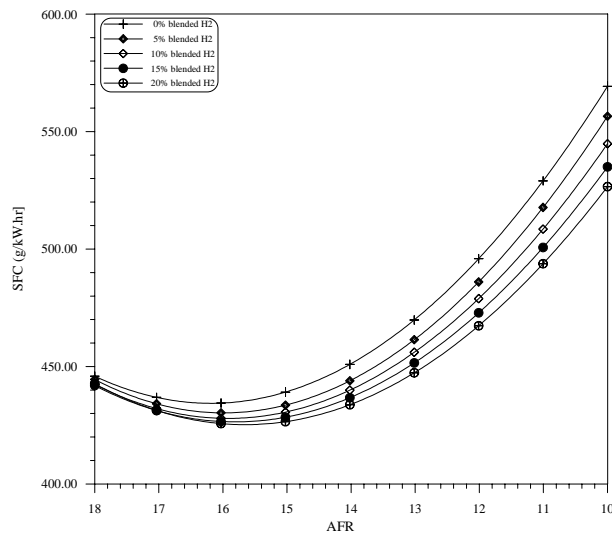


Figure (14) The Effect of AFR on IMEP for Different Hydrogen Blending Ratio
AFR=14, 2000 rpm, C.R.=6.5



Figure(6.59) The Effect of air to fuel ratio on Engine Power for Different Hydrogen Blending Ratio at 2000 rpm, C.R.=6.5 (naturally aspirated)

Figure (15) The Effect of AFR on Power for Different Hydrogen Blending Ratio
AFR=14, 2000 rpm, C.R.=6.5



Figure(6.60) The Effect of air to fuel ratio on SFC for Different Hydrogen Blending Ratio at 2000 rpm, C.R.=6.5 (naturally aspirated)

Figure (16) The Effect of AFR on SFC for Different Hydrogen Blending Ratio
AFR=14, 2000 rpm, C.R.=6.5

References

1. Y. Liu, K. C. Midkiff, and S. R. Bell, "Development of a Multizone Model for Direct Injection Diesel Combustion", Int. Journal of Engine Res., vol. 5, No. 1, pp. 71-81, 2003.

2. G. P. Parbhu, B. Nagalingam and K. V. Gopalakrishnan, "Theoretical Study of a Spark Ignited Supercharged Hydrogen Engine", International Journal of Hydrogen Energy, vol. 10, No. 6 pp. 389-397, 1985. <http://www.elsevier.com/locate/ijhydene>
3. Haroun A. K. Shahad and Maher S. AL-Baghdadi, "A Prediction Study of the Effect of Hydrogen Blending on the Performance and Pollutants Emission of a Four Stroke Spark Ignition Engine", International Journal of Hydrogen Energy, vol. 24, pp. 783-793, 1999. <http://www.elsevier.com/locate/ijhydene>
4. L.M. Das, R. Gulati, and P.K. Gupta, "A Comparative of the Performance Characteristics of a Spark Ignition Engine Using Hydrogen and Compressed Natural Gas as Alternative Fuels", International Journal of Hydrogen Energy, vol. 25, pp. 363-375, 2000. <http://www.elsevier.com/locate/ijhydene>
5. Ghazi A. Karim, "Hydrogen as a Spark Ignition Engine Fuel", International Journal of Hydrogen Energy, vol. 28, pp. 569-577, 2003. <http://www.elsevier.com/locate/ijhydene>
6. Le Corre Olivier, and Pirotais Frederic, "NO_x Emission Reduction of a Natural Gas SI Engine Under Lean Conditions: Comparison of the EGR and RGR Concepts", Proceedings of ICES, 2006 Spring Technical Conference, of the ASME Internal Combustion Engine Division, Aachen, Germany, May 8-10, 2006.
7. J. F. Cassidy, "Emission and Total Energy Consumption of a Multi cylinder Piston Engine Running on Gasoline and a Hydrogen – Gasoline Mixture", Nasa Technical Note, Nasa TN D-8487, National Aeronautics and Space Administration, Washington, D. C. May, 1977.
8. S. Furuham, and Y. Kobayashi, "A Liquid Hydrogen Car With A Two – Stroke Direct Injection Engine and LH₂ – Pump", International Journal of Hydrogen Energy, vol. 7, No. 10 pp. 809-820, 1982. <http://www.elsevier.com/locate/ijhydene>
9. F. E. Lynch, "Parallel Induction: A Simple Fuel Control Method for Hydrogen Engines", International Journal of Hydrogen Energy, vol. 8, No. 9 pp. 721-730, 1983. <http://www.elsevier.com/locate/ijhydene>
10. B. Haragopala, K. N. Shrivastava and H. N. Bhakta, "Hydrogen for Dual Fuel Engine Operation", International Journal of Hydrogen Energy, vol. 8, No. 5 pp. 381-384, 1983. <http://www.elsevier.com/locate/ijhydene>
11. K. S. Varde, and G. A. Frame, "Hydrogen Aspiration in a Direct Injection Type Diesel Engine – Its Effect on Smoke and Other Engine Performance Parameters",

International Journal of Hydrogen Energy, vol. 8, No. 7 pp. 549-555, 1983.

<http://www.elsevier.com/locate/ijhydene>

12. Samir M. Abdulhaleem, "Theoretical and experimental investigation of engine performance and emissions of a four stroke spark ignition engine operated with hydrogen blended gasoline". Ph.D. thesis, Al-Mustansiriya University, Baghdad, Iraq, 2007.
13. M. F. Modest, "Radiative Heat Transfer" Copyright by McGraw-Hill, 1993.
14. M. N. Ozisik, "Heat Transfer, a Basic Approach" Copyright by McGraw-Hill, 1988.
15. M. A., Al-Baghdadi, "The Effect of Hydrogen Addition on the Performance and Emissions of a Four Stroke Spark Ignition Engine" M.SC. Thesis, University of Babylon, 1996.
16. H., Hayami, et al, "Application of a Low Solidity Cascade Diffuser to Transonic Centrifugal Compressor" Tran. ASME, vol.112, pp.25-29, January 1990.
17. J. D., Mattingly, "Element of Gas Turbine Propulsion" Copyright by McGraw-Hill, 1996.
18. J. B., Heywood, "Internal Combustion Engine Fundamentals" Copyright by McGraw-Hill, 1989.
19. S. M. Abdul-Haleem, "Modeling of a Turbocharged Four Stroke Diesel Engine" M.SC. Thesis, University of Babylon, 2001.
20. G. H. Choi, Y. J. Chung, and S. B. Han, "Effect of Hydrogen Enriched LPG Fuelled Engine with Converted from a Diesel Engine", Proceedings International Hydrogen Energy Congress and Exhibition IHEC 2005, Istanbul, Turk